

# On the Characteristic Difference of Neoclassical Bootstrap Current and Its Effects on MHD Equilibria between CHS Heliotron/Torsatron and CHS-qa Quasi-Axisymmetric Stellarator

ISOBE Mitsutaka, OKAMURA Shoichi, NAKAJIMA Noriyoshi, SHIMIZU Akihiro<sup>1</sup>,  
NISHIMURA Shin, SUZUKI Chihiro, MURAKAMI Sadayoshi, FUJISAWA Akihide  
and MATSUOKA Keisuke

*National Institute for Fusion Science, Toki, Gifu 509-5292, Japan*

<sup>1</sup> *Nagoya University, Nagoya, Aichi 464-8603, Japan*

(Received: 11 December 2001 / Accepted: 17 May 2002)

## Abstract

The characteristic difference of neoclassical bootstrap current and its effects on MHD equilibria are described for the CHS heliotron/torsatron and the CHS-qa quasi-axisymmetric stellarator. The direction of bootstrap current strongly depends on collisionality in CHS, whereas it does not in CHS-qa because of quasi-axisymmetry. In the CHS configuration, it appears that enhanced bumpy ( $B_{01}$ ) and sideband components of helical ripple ( $B_{11}$ ) play an important role in reducing the magnetic geometrical factor, which is a key factor in evaluating the value of bootstrap current, and determining its polarity. The bootstrap current in CHS-qa is theoretically predicted to be larger than that in CHS and produces significant effects on the resulting rotational transform and magnetic shear. In the finite  $\beta$  plasmas, the magnetic well becomes deeper in both CHS and CHS-qa and its region is expanded in CHS. The existence of co-flowing bootstrap current makes the magnetic well shallow in comparison with that in currentless equilibrium.

## Keywords:

quasi-axisymmetric stellarator, heliotron/torsatron, geometrical factor, bootstrap current

## 1. Introduction

In recent years, many theoretical and computational efforts have been made to explore advanced stellarator configurations [1-5] and as a result, new stellarator concepts such as quasi-isodynamicity, quasi-helical symmetry, and quasi-axisymmetry have been proposed. A basic idea in developing new types of stellarators is to realize configurations having magnetohydrodynamically stable characteristics as well as good neoclassical confinement.

In the National Institute for Fusion Science, the

Compact Helical System (CHS) experiment has been undertaken to investigate the confinement properties of low aspect ratio ( $A_p \sim 5$ ) heliotron/torsatron plasmas. In order to explore further good confinement regime of a compact stellarator, we propose a quasi-axisymmetric stellarator CHS-qa as a post-CHS device [6-9]. The primary concept of CHS-qa is to be MHD stable and to improve trapped particle orbits with realizing a tokamak-like, quasi-axisymmetric magnetic field configuration on the Boozer coordinates and

---

Corresponding author's e-mail: [isobe@nifs.ac.jp](mailto:isobe@nifs.ac.jp)

maintaining the compactness, which is the policy of CHS. In CHS-qa, the magnetic well is realized in the entire plasma region and neoclassical transport is largely improved compared with that in CHS. Moreover, in actual experiments, the quasi-axisymmetry may lead to a drastically improved confinement regime such as that observed in tokamaks.

One of the remarkable differences between CHS and CHS-qa concerns the bootstrap current property. In tokamaks, the bootstrap current is recognized to be very important in regard to the steady state operation. Although this current is not essentially required for confining helical plasmas, it is important in helical systems because it certainly affects not only MHD equilibrium and stability but also transport and trajectories of energetic ions through the change of the rotational transform  $1/2\pi$  and magnetic field spectra. Neoclassical theory predicts that the bootstrap current behavior is complicated in CHS. The direction of bootstrap current can be changed from co- to counter-, and vice versa, depending on collisionality and magnetic field structure, which can be changed through magnetic axis position  $R_{ax}$  and/or the ellipticity of the plasma cross section. On the other hand, in CHS-qa, bootstrap current always flows co-directionally and its magnitude is predicted to be larger than that in CHS because of quasi-axisymmetry, resulting in much lower neoclassical viscosity. In this article, we compare neoclassical bootstrap current properties of CHS and CHS-qa in terms of the magnetic geometrical factor. In addition, the effects of bootstrap current on MHD equilibria are also discussed for both CHS and CHS-qa configurations.

## 2. Bootstrap Current Property in CHS and CHS-qa

### 2.1 Basic Features of CHS and CHS-qa

CHS is a low aspect ratio ( $R/a \sim 5$ ) heliotron/torsatron device with a toroidal period number of  $N = 8$  and polarity  $l = 2$  [10]. The device's major radius  $R$  is 1 m. The magnetic field is produced by two helical winding coils and three sets of poloidal coils. CHS is flexible in its wide variability of  $R_{ax}$  and ellipticity of the plasma cross section. The toroidal magnetic field  $B_t$  can be increased up to 2 T. The CHS experiment began in 1988 and we have studied confinement properties of low aspect ratio ( $R/a \sim 5$ ) heliotron/torsatron plasmas. CHS-qa is a quasi-axisymmetric stellarator with  $N = 2$ .  $R$  is 1.5 m and its aspect ratio is fairly low,  $R/a = 3.2$  in the present design. The magnetic field is produced by twenty modular coils, which are capable of a maximum  $B_t$  of 1.5 T [11]. Three sets of poloidal coils and eight additional toroidal coils will be equipped to control the properties of a magnetic field configuration such as  $R_{ax}$ ,  $1/2\pi$  and the magnetic well depth. Figure 1 shows the magnetic field spectra of the vacuum magnetic field of both CHS and CHS-qa. In an inwardly shifted configuration of CHS ( $R_{ax} = 0.921$  m), the magnetic field structure is dominated by  $B_{10}$  (toroidicity) and  $B_{21}$  (helical ripple) (see Fig. 1(a)). The amplitude of  $B_{21}$  steeply increases toward the plasma boundary. It should be noted that there is a  $B_{10}$ -dominated structure in the core domain. An outwardly shifted configuration ( $R_{ax} = 0.995$  m) has a more complicated magnetic field structure than that in  $R_{ax}$  of 0.921 m. In addition to  $B_{10}$  and  $B_{21}$ ,  $B_{11}$  (the sideband component of a helical ripple)

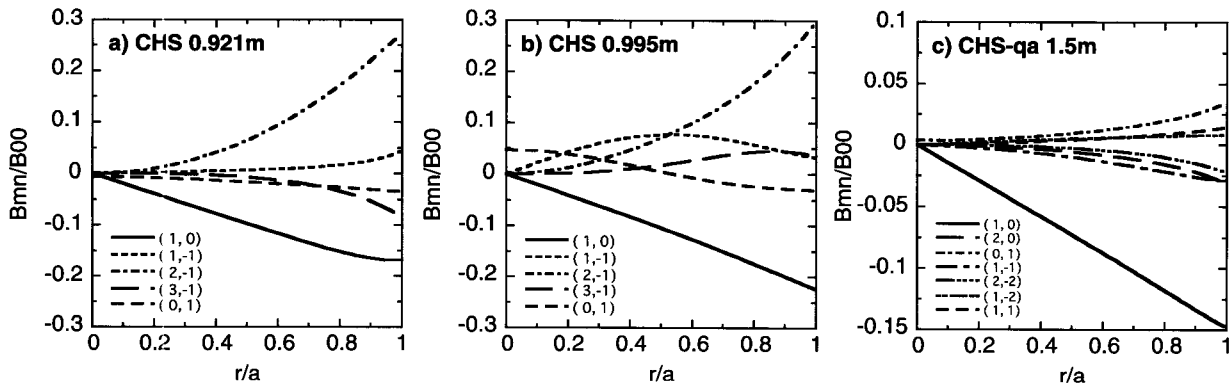


Fig. 1 Magnetic field spectra on the Boozer coordinates in vacuum configurations. (a) CHS ( $R_{ax} = 0.921$  m), (b) CHS ( $R_{ax} = 0.995$  m), and (c) CHS-qa.

and  $B_{01}$  (bumpiness) are largely enhanced especially in the core domain (see Fig. 1(b)). The magnetic field structure of CHS-qa is quite different from that of CHS. In CHS-qa, a tokamak like,  $B_{10}$ -dominated magnetic field structure is achieved in the whole region (see Fig. 1(c)), although residual non-axisymmetric magnetic field components still exist in the peripheral region. The profiles of  $1/2\pi$  and magnetic well depth of CHS and CHS-qa are shown in Sec. 3 in detail.

### 2.2 Magnetic Geometrical Factor

The neoclassical bootstrap current density  $j_{bs}$  of a non-axisymmetric helical system in the banana ( $1/\nu$ ) regime is scaled as [12,13],

$$\langle j_{bs} B \rangle_s \propto (f_i/f_c) G_{bs}^{banana} P (n'/n + \alpha_1 T_i'/T_i + \alpha_2 T_e'/T_e)$$

The bootstrap current is calculated in terms of the magnetic geometrical factor  $G_{bs}$ .  $B$  is the magnetic field strength and  $\langle \rangle_s$  denotes the flux surface average.  $\alpha_1$  and  $\alpha_2$  are constants, and  $f_i$  and  $f_c$  are the fractions of trapped particles and circulating particles, respectively.  $P$ ,  $n$ ,  $T_e$  and  $T_i$  are the total pressure ;  $P = n_e T_e + n_i T_i$ , density, electron temperature, and ion temperature, respectively. The primes stand for  $d/d\psi$ ,  $\psi = \phi_T/2\pi$  where  $\phi_T$  is the toroidal flux. Figure 2 shows the ratio of  $G_{bs}$  of CHS and CHS-qa to that of an equivalent tokamak,  $G_{bs}/G_{bs}^{tok}$  for vacuum magnetic fields in the banana and pla-

teau regimes. The magnitude and polarity of  $G_{bs}$  is sensitive to  $R_{ax}$  and the collisionality regime in CHS. Figure 2(a) suggests that in CHS, the neoclassical bootstrap current flows in the co-direction if the plasma is in the banana regime. The  $B_{10}$ -dominated structure in the core domain of  $R_{ax} = 0.921$  m gives large  $G_{bs}^{banana}$ , which is comparable to that in CHS-qa. On the other hand, in  $R_{ax}$  of 0.995 m, the magnitude of  $G_{bs}^{banana}$  in the core domain is much smaller than that in  $R_{ax}$  of 0.921 m. Judging from Figure 1(b), it is supposed that augmented amplitude of  $B_{01}$  and  $B_{11}$  plays an important role in reducing the value of  $G_{bs}^{banana}$ . If the CHS plasma is in the plateau regime, the magnitude of  $G_{bs}^{plateau}$  becomes smaller than that of  $G_{bs}^{banana}$  and the direction of the bootstrap current can be switched from the co- to the counter-direction. Especially, at  $R_{ax}$  of 0.995 m, the polarity of  $G_{bs}^{plateau}$  is opposite in the whole region to that of  $G_{bs}^{banana}$ . This means that in the plateau regime, the bootstrap current flows in the counter-direction in the whole region of a plasma having  $R_{ax} = 0.995$  m. The magnitude of  $G_{bs}$  in CHS-qa is larger than that in CHS and its polarity does not depend on the collisionality regime. The significant difference from CHS is that there is no large difference in the magnitude of  $G_{bs}$  between the banana and plateau regimes. The neoclassical theory predicts that in CHS-qa, the bootstrap current is larger than that in CHS and always flows in the co-direction. It should be noted that the ratio  $G_{bs}/G_{bs}^{tok}$  is not very close to 1 in CHS-qa because of the residual non-

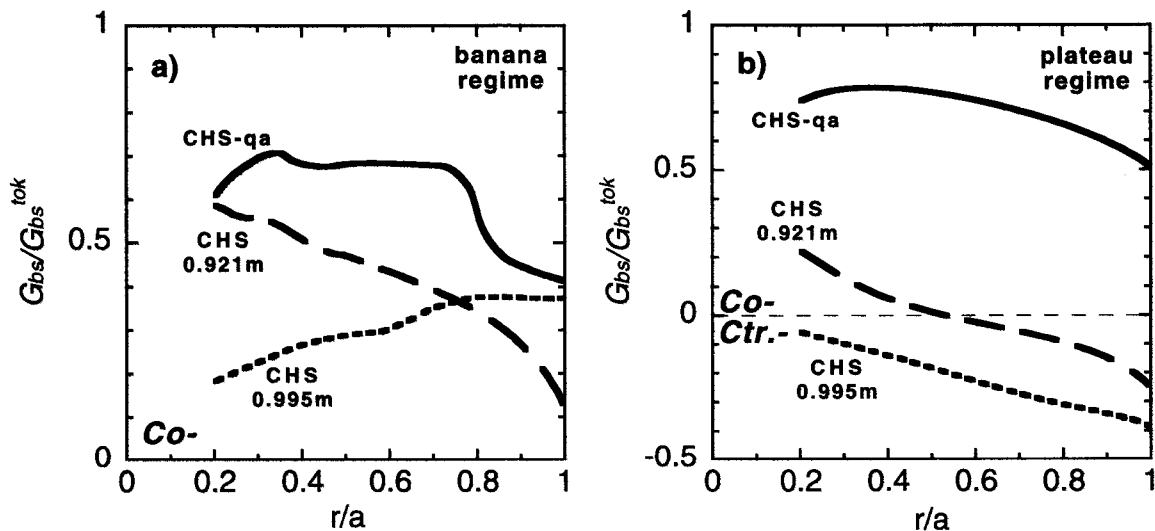


Fig. 2 Magnetic geometrical factors in vacuum configurations. (a) CHS ( $R_{ax} = 0.921$  m), (b) CHS ( $R_{ax} = 0.995$  m), and (c) CHS-qa.

axisymmetric magnetic field components.

### 3. Effects of Bootstrap Current on MHD Equilibrium

In order to investigate the effects of bootstrap current on finite  $\beta$  equilibria of both CHS and CHS-qa, the SPBSC code which calculates the three-dimensional MHD equilibrium including neoclassical bootstrap

current self-consistently in the whole collisionality range from the banana to the Pfirsch-Schlüter regime [14] has been employed. It has been so far confirmed that this code reproduces well the experimental bootstrap currents in ECRH plasmas of CHS at moderate density ( $n_e \sim 1.0 \times 10^{19} \text{ m}^{-3}$ ) [15,16]. Figure 3 shows the profiles of bootstrap current density  $dI_{bs}/ds$ ,  $i/2\pi$  and magnetic well depth in the vacuum and finite  $\beta$  equilibria of CHS

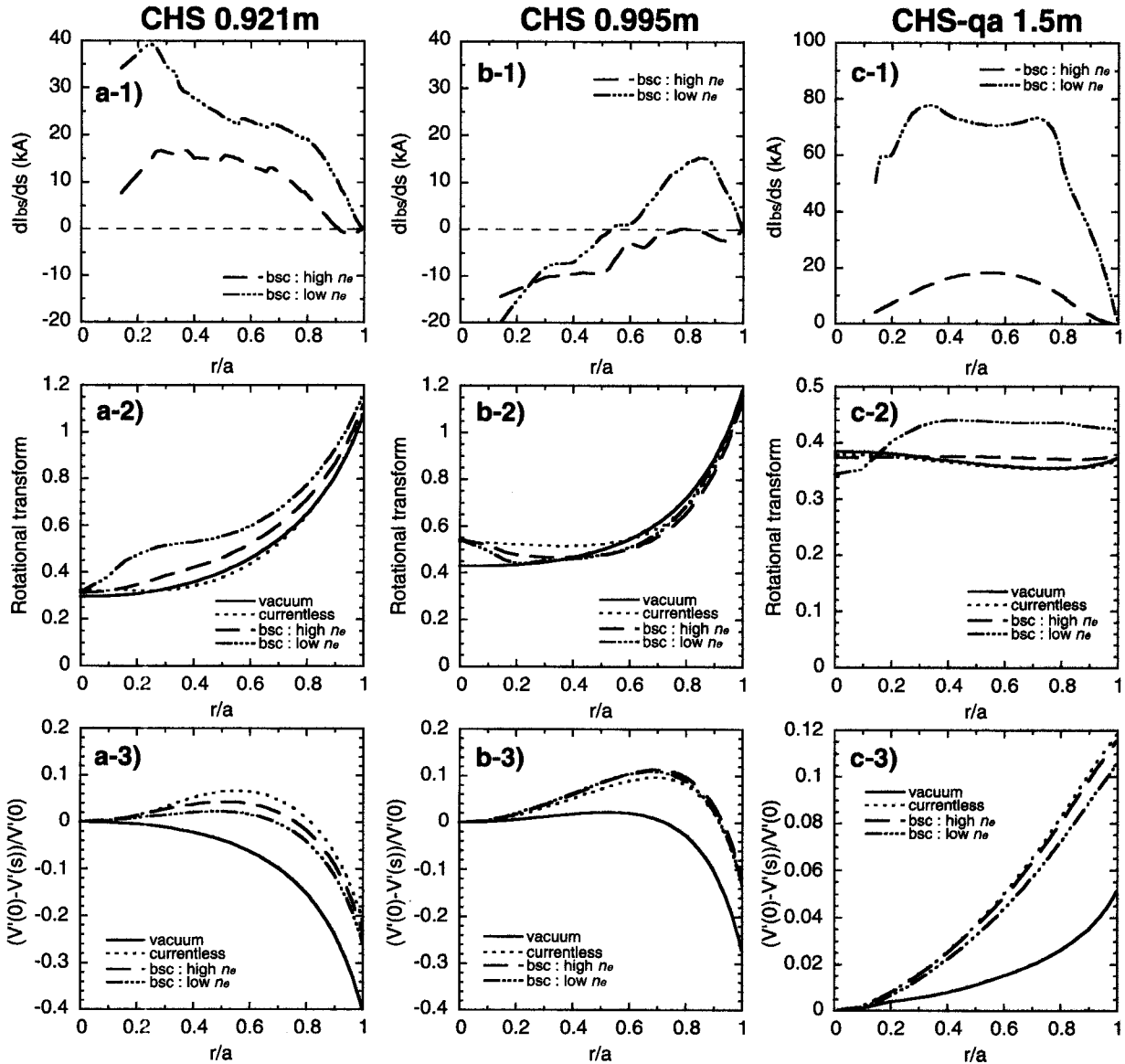


Fig. 3 Bootstrap current density, rotational transform, and magnetic well depth in the vacuum, currentless finite  $\beta$  equilibrium, and finite  $\beta$  equilibrium including neoclassical bootstrap current self-consistently for high  $n_e$  ( $n_e(0) = 1.0 \times 10^{20} \text{ m}^{-3}$ ) and low  $n_e$  ( $n_e(0) = 2.0 \times 10^{19} \text{ m}^{-3}$ ) cases. (a) CHS ( $R_{ax} = 0.921 \text{ m}$ ), (b) CHS ( $R_{ax} = 0.995 \text{ m}$ ), and (c) CHS-qa. The central beta value  $\beta(0)$  is 2.8%. The calculations were carried out under the fixed boundary condition. The radial electric field  $E_r$  was not taken into account.

( $R_{ax} = 0.921$  m,  $0.995$  m) and CHS-qa. The calculations of MHD equilibria were performed for the following four cases ; 1) vacuum, 2) currentless finite  $\beta$ , 3) finite  $\beta$  with self-consistently including bootstrap current in high  $n_e$  case, and 4) in low  $n_e$  case. The plasma parameters used here are ;  $T_e(0) = 0.4$  keV,  $T_i(0) = 0.3$  keV, and  $n_e(0) = n_i(0) = 1.0 \times 10^{20}$  m $^{-3}$  for high  $n_e$  case,  $T_e(0) = 2.0$  keV,  $T_i(0) = 1.5$  keV, and  $n_e(0) = n_i(0) = 2.0 \times 10^{19}$  m $^{-3}$  for low  $n_e$  case with profiles of  $T = T(0)(1 - s)$ ,  $n = n(0)(1 - 0.8s + 1.3s^2 - 1.5s^3)$ , and  $B_t = 1$  T. Here,  $s$  is the label representing the normalized toroidal flux. The  $n_e$  gradually declines toward  $s = 0.9$  and then rapidly drops to zero toward the plasma boundary ( $s = 1$ ). These parameters give a central  $\beta$  value of  $\beta(0) = 2.8$  %. The normalized collision frequency  $\nu^*$  in low and high  $n_e$  cases for both inwardly and outwardly shifted configurations of CHS are  $(1 - 2) \times 10^{-2}$  and  $1.5 - 3$  at  $r/a (= s^{1/2})$  of  $0.7$ , respectively. For CHS-qa,  $\nu^*$  is  $\sim 0.4$  for low  $n_e$  and  $\sim 50$  for high  $n_e$ . Here, the condition of  $\nu^* \ll 1$  and  $\nu^* \gg 1$  correspond to the limit of the  $1/\nu$  regime and of the plateau regime, respectively. The plasma potential is not considered in this analysis.

In  $R_{ax}$  of  $0.921$  m, the neoclassical bootstrap current flows co-directionally in both low and high  $n_e$  cases (see Fig. 3(a-1)) and increases  $i/2\pi$  as a result (see Fig. 3(a-2)). The total bootstrap currents  $I_{bs}$  for low and high  $n_e$  cases are  $+20$  kA and  $+8.7$  kA, respectively. Here, “+” indicates the co-direction, while “-” represents the counter-direction. There is no magnetic well region in the vacuum configuration of  $R_{ax} = 0.921$  m, but in the finite  $\beta$  case, the magnetic well is formed in the region of  $r/a < 0.6$  due to a Shafranov shift. It is seen that the bootstrap current suppresses the formation of the magnetic well compared with the currentless equilibrium because it pushes up  $i/2\pi$  and then reduces the Shafranov shift. In finite  $\beta$  plasmas of an outwardly shifted configuration ( $R_{ax} = 0.995$  m),  $I_{bs}$  for low and high  $n_e$  plasmas are  $+4.1$  kA and  $-3.9$  kA, respectively. The bootstrap current in the high collisionality plasma flows in the counter-direction over the whole region as expected from Fig. 2. It is interesting to note that in the low collisionality plasma, the bootstrap current flows in opposite directions at the center and edge. As discussed in Sec. 2.2, in the vacuum equilibrium, the direction of the bootstrap current in the core domain is expected to be co- in the low collisionality regime, whereas the self-consistent bootstrap calculation for finite  $\beta$  equilibrium in the low collisionality case shows that the direction of the current in the core domain is in counter-direction. The  $B_{01}$  component is augmented, by about double at the

plasma center and the  $B_{11}$  component is also slightly increased in the finite  $\beta$  equilibrium in comparison with those in the vacuum equilibrium. In  $R_{ax}$  of  $1.106$  m, which is the most outwardly shifted configuration of CHS, the amplitude of  $B_{01}$  and  $B_{11}$  in the vacuum is larger than that in the finite  $\beta$  equilibrium of  $R_{ax} = 0.995$  m and the polarity of  $G_{bs}^{banana}$  is negative in the domain of  $r/a < 0.45$ . Based on these facts, the counter-flowing bootstrap current seen in Fig. 3(b-1) is supposed to be due to augmented  $B_{01}$  and  $B_{11}$  components. A similar discussion is available in ref. [13] for the Large Helical Device (LHD), which has a magnetic field configuration analogous to that of CHS. The effect of counter-directed bootstrap current on  $i/2\pi$  is clearly seen in the core domain (see Fig. 3(b-2)) and plays a desirable role in expanding magnetic well region (see Fig. 3(b-3)) from the viewpoint of MHD stability. In CHS-qa, the bootstrap current always flows co-directionally (see Fig. 3(c-1)), increasing  $i/2\pi$ . In the low  $n_e$  case,  $I_{bs}$  is  $+56$  kA and exerts significant effects on  $i/2\pi$  profile.  $I_{bs}$  of  $+10.6$  kA in the high  $n_e$  case effects the value of  $i/2\pi$  less but it produces almost no magnetic shear. It should be mentioned that in CHS-qa,  $i/2\pi$  tends to decrease as  $\beta$  increases in the currentless equilibrium, therefore it is very important to take into account of bootstrap current in the finite  $\beta$  equilibrium.  $I_{bs}$  steeply increases as  $\beta$  increases, reaching  $100$  kA when  $\langle\beta\rangle$  exceeds  $2\%$  in the low collisionality regime [17]. The effect of finite  $\beta$  on magnetic well depth is very clear. It enhances the magnetic well from  $5\%$  (vacuum) to more than  $10\%$  (finite  $\beta$ ) at the plasma boundary. The co-flowing bootstrap current and resulting higher  $i/2\pi$  make the magnetic well shallower than that in the currentless finite  $\beta$  equilibrium through suppression of the Shafranov shift.

#### 4. Summary

We have investigated the collisionality and  $R_{ax}$  dependence of the bootstrap current properties and their effects on MHD equilibria for CHS heliotron/torsatron and CHS-qa quasi-axisymmetric stellarator. It was shown that the behavior of bootstrap current is complicated in CHS. Especially in the outwardly shifted configuration, the bootstrap current can easily change its direction from co- to counter-, and vice versa, depending on collisionality. The analyses of magnetic field spectra suggest that the enhanced amplitude of  $B_{01}$  and  $B_{11}$  components plays an important role in reducing the magnitude of  $G_{bs}$ . Judging from the magnitude and polarity of  $G_{bs}$ , a larger bootstrap current, which always

flows in the co-direction, is predicted in CHS-qa because of quasi-axisymmetry and the  $\iota/2\pi$  profile is significantly affected by the existence of bootstrap current especially in the low collisionality high  $\beta$  regime. In regard to the effect of finite  $\beta$  on the magnetic well, it results in forming and expanding the magnetic well region in CHS. In CHS-qa, the magnetic well is realized in the whole plasma domain in the vacuum equilibrium and becomes deeper as  $\beta$  increases. It is clearly shown that the existence of co-flowing bootstrap current reduces the magnetic well depth compared with that of currentless finite  $\beta$  equilibrium for both configurations. Therefore, we see that it is important to consider MHD equilibrium including self-consistent bootstrap current for physics design studies of a new stellarator CHS-qa.

### Acknowledgments

We are grateful to Profs M. Fujiwara and O. Motojima for their continuous encouragement. One of the authors (MI) thanks Dr. K.Y. Watanabe for the use of the SPBSC code.

### References

- [1] J. Nührenberg and R. Zille, *Phys. Lett.* **114A**, 129 (1986).
- [2] J. Nührenberg and R. Zille, *Phys. Lett. A* **129**, 113 (1988).
- [3] J. Nührenberg, W. Lots and S. Gori, *Theory of Fusion Plasmas Varrenna* 1994, 3 (Ed. Comp., Bologna, 1994).
- [4] A. Reiman *et al.*, *Plasma Phys. Control. Fusion* **41**, B273 (1999).
- [5] D.A. Spong *et al.*, *Phys. Plasmas* **5**, 1752 (1998).
- [6] K. Matsuoka *et al.*, *Plasma Physics Reports* **23**, 542 (1997).
- [7] S. Okamura *et al.*, *J. Plasma Fusion Res. SERIES* **1**, 164 (1998).
- [8] S. Okamura *et al.*, in *Plasma Physics and Controlled Nuclear Fusion Research 2000 (Proc. 18th Int. Conf. Sorrent, 2000)* IAEA-CN-77/ICP/16.
- [9] K. Matsuoka *et al.*, *J. Plasma Fusion Res. SERIES* **4**, 111 (2001).
- [10] K. Matsuoka *et al.*, in *Plasma Physics and Controlled Nuclear Fusion Research 1988 (Proc. 12th Int. Conf. Nice, 1988)*, Vol.2, IAEA, Vienna, 411 (1989).
- [11] A. Shimizu *et al.*, *submitted to Fusion Eng. Design.*
- [12] K.C. Shaing and J.D. Callen, *Phys. Fluids* **26**, 3315 (1983).
- [13] K.Y. Watanabe and N. Nakajima, *Nucl. Fusion* **41**, 63 (2001).
- [14] K.Y. Watanabe *et al.*, *Nucl. Fusion* **35**, 335 (1995).
- [15] H. Yamada *et al.*, *Nucl. Fusion* **34**, 641 (1994).
- [16] M. Isobe *et al.*, *Plasma Phys. Control. Fusion.* **44** (2002) A189-A195.
- [17] M. Isobe *et al.*, *28th EPS Conference on Contr. Fusion and Plasma Phys. Funchal*, 18–22 June 2001, ECA Vol.25A (2001) 761–764.